PARAMETRIC INVESTIGATION OF CONJUGATE HEAT TRANSFER FROM MICROELECTRONIC CIRCUIT BOARDS UNDER MIXED CONVECTION COOLING

BY

S. Lee[1], J.R. Culham[2] and M.M. Yovanovich[3]

Microelectronics Heat Transfer Laboratory
Department of Mechanical Engineering
University of Waterloo
Waterloo, Ontario, Canada N2L 3G1

Abstract

The attention given to thermal considerations in the design and manufacture of microelectronic equipment has gained more prominence in recent years primarily due to stringent reliability constraints which must be maintained despite ever increasing packaging densities and power dissipation levels. If design simplicity is to be maintained, effective yet complex cooling techniques such as fins, microchannels and jet impingement will be avoided unless absolutely necessary. In light of this, an examination of the fundamental design options facing circuit designers is presented in this paper.

A dimensional analysis of the governing equations for conjugate mixed convection heat transfer is presented in order to determine the dimensionless parametric groups which contribute to heat transfer. META - an analytical/numerical conjugate heat transfer model is used to calculate temperature distributions in a test circuit board which is assumed to have low profile, flush mounted heat sources. Design options, such as the thermal conductivity and surface emissivity of the circuit board, the flow velocity of the cooling fluid and the positioning and power dissipation of the heat sources are examined here in order to determine the relative merit of each as a means of controlling circuit board temperatures. The thermal response of the circuit board to changes in each of these design parameters is assessed over a range of conditions typically observed in microelectronics applications.

[1]Research Assistant Professor, Member IEPS
[2]Assistant Director
[3]Professor and Director, Member IEPS

Nomenclature

Bi	Biot number $\equiv ht/k_s$
Bq	Boussinesq number $\equiv g\beta L^4 q/(k_f \alpha^2)$
$\tilde{d}$	dimensionless distance between heat sources
g	gravitational acceleration, m^2/s
h	heat transfer coefficient, $\mathrm{W/(m^2 \cdot K)}$
k	thermal conductivity, $\mathrm{W/(m \cdot K)}$
ℓ	heat source length and width, m
L	total circuit board length, m
Nu_2	Average Nusselt Number of second heat source $\equiv Q_{j_2}/((\overline{T_2} - T_\infty) \cdot k_f \cdot \ell)$
Pe	Peclet number $\equiv u_\infty \cdot L/\alpha$
Pr	Prandtl number $\equiv \nu/\alpha$
q	heat flux density, $\mathrm{W/m^2}$
Q	heat dissipation, W
t	board thickness, m
T	temperature, K
u, v, w	boundary layer velocity in the x, y and z-direction, respectively, m/s
u_∞	free stream velocity, m/s
W	circuit board width, m
x, y, z	Cartesian coordinates

Greek Symbols

α	thermal diffusivity $\equiv k_f/(\rho \cdot c_p)$, $\mathrm{m^2/s}$
β	thermal expansion coefficient, K^{-1}
ϵ	emissivity
ϕ	relative temperature change in the downstream heat source $\equiv (\Delta T_2 - \Delta T_{2,0})/\Delta T_{2,0}$
θ	dimensionless temperature excess $\equiv (T - T_\infty)/\Delta T_{ref}$
ν	kinematic viscosity, m^2/s
σ	Stefan-Boltzmann constant $\equiv 5.67 \times 10^{-8}$, $\mathrm{W/(m^2 \cdot K^4)}$

Subscripts

c	circuit board center line
f	fluid
f	forced
j	Joulean
max	maximum
r_1, r_2	radiation from the front and back surfaces, respectively
ref	reference
s	solid
sk	sink
w_1, w_2	front and back wall, respectively
∞	free stream

Superscripts

*	dimensionless variable

Introduction

The prediction of circuit board and IC junction operating temperatures, heat flux distributions and heat transfer coefficients necessitates the use of a conjugate, mixed convection heat transfer model to fully account for the complex phenomena occurring during the cooling process. The interaction between the temperature field established in the circuit board and the components on the surface of the circuit board must be considered simultaneously with the temperature field established in the surrounding boundary layer. All modes of heat transfer must be considered, including conduction within the circuit board and its components, convection, whether natural, forced or a combined mixed mode and radiation from the surface of the circuit board to the surrounding circuit boards or containment unit.

Computer Aided Design (CAD) tools based on finite element or finite difference techniques are often used to perform the rigorous thermal assessment required throughout the many design processes required in the development of microelectronic circuit boards. However, the numerous tradeoff studies performed during the initial stages of the design process restrict the use of most numerically based CAD tools because of the cost involved in setting up and running parametric studies. Although the wealth of output data available from most state-of-the-art CAD tools is of great interest to a select few, most designers do not need detailed heat transfer information, especially during the early stages of the design process where upper and lower bounds on operating conditions are sufficient for most design decisions. These bounds can be based on empirically derived data, analytical approximations or as in the case of this paper, the presentation of a case study where a specific example is examined in some detail to ascertain a better understanding of the relationship between basic design parameters and conjugate heat transfer.

Thermal Model

An analytical/numerical model - META (Culham et al., 1991b) is used to simulate conjugate heat transfer in a microelectronic circuit board, as shown in Fig. 1. The circuit board consists of a multilayered substrate, made up of alternating layers of highly conductive materials such as copper tracking and layers of insulating materials such as fiberglass/epoxy. The enlarged illustration in Fig. 1 shows a side view of the circuit board/heat source interface where the pertinent modes of heat dissipation involved in liberating heat from the IC junction to the surrounding cooling fluid are shown.

As mentioned above, heat transfer problems pertaining to microelectronic applications can become extremely cumbersome unless several simplifying assumptions are incorporated. The following assumptions, used in the analytical modeling, significantly simplify the modeling process but do not detract from the accuracy or the physical integrity of the final solution.

1. Low profile, flush mounted heat sources are assumed to be in perfect contact with the printed circuit board. Sources of this type are representative of chip-on-board or surface mount technology.

2. The circuit board aspect ratio, defined as the total length of the board in the flow direction over the thickness of the board (L/t), is of the order 125:1. The predominant surfaces for convective cooling are the front and back surfaces of the circuit board, which encompass approximately 99% of the total exposed surface area of the board. Therefore, the heat transfer through the edges of the board is considered negligible and these surfaces will be treated as adiabatic.

3. Although the convective heat transfer coefficient varies significantly over the surface of an electronic

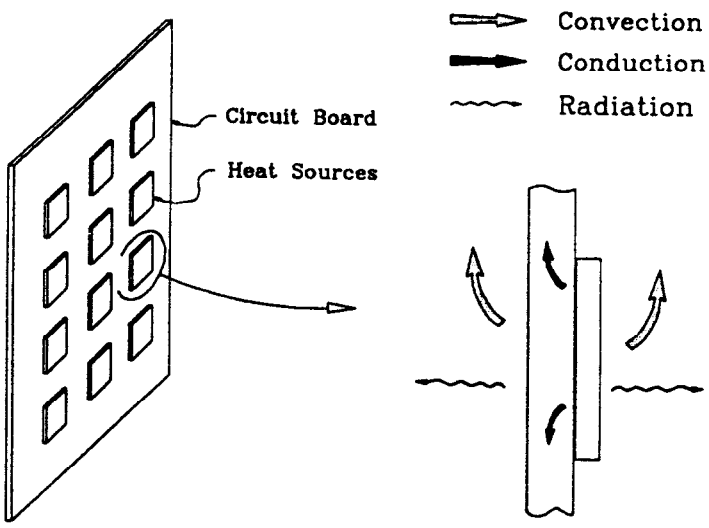

Figure 1: Conjugate Heat Transfer From a Printed Circuit Board With Surface Mounted Packages

circuit board, cooled by mixed convection, typical values of the Biot Number ($\mathrm{Bi} = ht/k_s$) range from 0.001 to 0.1. The Biot number serves as an indication of the relative magnitude of the thermal resistance across the thickness of the board to the thermal resistance within the fluid boundary layer. Since it is commonly accepted that a $\mathrm{Bi} < 0.1$ allows a two-dimensional conduction analysis to be used with minimal deviation from results obtained using a more rigorous three-dimensional solution, a two-dimensional model will be used in this analysis.

4. The cooling fluid is taken to be dry air with flow over the circuit board assumed to be steady, two dimensional and incompressible.

5. The power dissipated by the components is assumed to be steady and invariant with respect to time.

Fluid-Side Equations

The standard boundary layer equations, in which the transport of momentum and energy by diffusion processes is assumed negligible compared to convection in the direction parallel to the flow stream, will be used to describe the flow and energy field within the surrounding fluid. The v-velocity in the y-direction, across the width of the circuit board, is small compared to both the applied forced flow and the buoyancy induced u-velocity in the x-direction. This, combined with a scale analysis, indicates that the convective transport in the y-direction can be ignored.

The thermophysical properties of the fluid, except the density variation used in the Boussinesq approximation, are assumed constant. The work done by the viscous force and the pressure work term are neglected. When air is used as a coolant fluid, its thermal conductivity ($\approx 0.03\ W/(m \cdot K)$) is usually orders of magnitude smaller than that of the circuit board. As such, one can assume that the planar thermal

diffusion parallel to the board surface (i.e., the x and y directions) is predominantly characterized by the conduction heat transfer in the circuit board. This not only supplements the validity of the boundary layer approximations but also allows one to ignore the planar diffusion of energy in the fluid, which in turn allows the planar diffusion of momentum to be ignored. Since the circuit board is thin and heat sources are usually mounted away from the edges of the circuit board, it is reasonable to assume that the operating temperature and the heat transfer characteristics of heating elements are not influenced by the edge effects. Based on the foregoing assumptions and approximations, the resulting governing equations become identical to the two-dimensional boundary layer equations in x-z coordinates.

$$\frac{\partial u}{\partial x} + \frac{\partial w}{\partial z} = 0 \tag{1}$$

$$u\frac{\partial u}{\partial x} + w\frac{\partial u}{\partial z} = \nu\frac{\partial^2 u}{\partial z^2} + g\beta(T - T_\infty) \tag{2}$$

$$u\frac{\partial T}{\partial x} + w\frac{\partial T}{\partial z} = \alpha\frac{\partial^2 T}{\partial z^2} \tag{3}$$

where the following boundary conditions are applied.

$$\text{as } z \to \infty \quad , \quad u \to u_\infty \quad , \quad T \to T_\infty \tag{4}$$

$$\text{at } x = 0 \quad , \quad u = u_\infty \quad , \quad T = T_\infty \tag{5}$$

$$\text{at } z = 0 \quad , \quad u = w = 0 \tag{6}$$

$$\text{at } z = -t \quad , \quad u = w = 0 \tag{7}$$

As mentioned above, these boundary conditions apply for all values of $0 \leq y \leq W$, where edge losses are assumed negligible.

Solid-Side Equations

The three-dimensional Laplace equation for heat flow in a homogeneous solid is

$$\frac{\partial^2 T}{\partial x^2} + \frac{\partial^2 T}{\partial y^2} + \frac{\partial^2 T}{\partial z^2} = 0 \tag{8}$$

where the boundary conditions along the edges of a flat plate, considered to be adiabatic, can be written as

$$\text{at } x = 0 \text{ and } L \qquad \frac{\partial T}{\partial x} = 0 \tag{9}$$

$$\text{at } y = 0 \text{ and } W \qquad \frac{\partial T}{\partial y} = 0 \tag{10}$$

The boundary conditions along the planar surfaces at the front surface of the board, denoted as $z = 0$, and the back surface of the board, denoted as $z = -t$ are given as

$$\text{at } z = -t \qquad T(z = -t^+) = T(z = -t^-) \tag{11}$$

$$k_s \left.\frac{\partial T}{\partial z}\right|_{-t^+} = q_{w_1} + q_{r_1} \tag{12}$$

$$\text{at } z = 0 \qquad T(z = 0^-) = T(z = 0^+) \tag{13}$$

$$k_s \left.\frac{\partial T}{\partial z}\right|_{0^-} = q_j - q_{w_2} - q_{r_2} \tag{14}$$

where q_{w_1} and q_{w_2} represent convective heat flux distributions over the front and back surfaces of the board, respectively and q_j denotes an input Joulean heat flux distribution which is obtained by dividing the total power input per heat source by the source area. The wall heat flux over both surfaces can be written as

$$q_{w_1} = k_f \left.\frac{\partial T}{\partial z}\right|_{-t^-} \tag{15}$$

$$q_{w_2} = -k_f \left.\frac{\partial T}{\partial z}\right|_{0^+} \tag{16}$$

The radiative heat flux distribution, q_{r_1} and q_{r_2}, from the front and back of the circuit board can be expressed in terms of the Boltzmann equation, as

$$q_{r_i} = \epsilon\sigma(T_{w_i}^4 - T_{sk}^4) \qquad \text{for } i = 1,\ 2 \tag{17}$$

where the emissivity is assumed constant over each surface.

If the Biot number ($\text{Bi} = ht/k_s$), which is a measure of the internal thermal resistance of the solid to the external thermal resistance within the boundary, is less than 0.1 then the temperature difference

across the thickness of the solid is small and a single average value of the cross sectional temperature can be used, thus reducing the dimensional dependency of the governing equation by a factor of one.

By integrating Laplace's equation across the thickness of the board, the interfacial conditions are absorbed into the governing equation, and Eqs. (8), (12) and (14) reduce to a two-dimensional fin equation

$$\frac{\partial^2 T}{\partial x^2} + \frac{\partial^2 T}{\partial y^2} + \frac{1}{k_s t}(q_j - q_r - q_w) = 0 \tag{18}$$

where $q_w = q_{w_1} + q_{w_2}$ and $q_r = q_{r_1} + q_{r_2}$.

The fluid and solid-side models described above are incorporated in a conjugate heat transfer modeling routine developed by the Microelectronics Heat Transfer Laboratory, entitled META (Culham et al., 1991b). META combines an analytical boundary layer solution with a finite volume solid body solution, as described in the preceding discussion. The boundary layer solution is based on a linearized form of the boundary layer equations (Lee and Yovanovich, 1991) for laminar flow over a flat plate with a flux specified boundary condition. The resulting formulation for the local Nusselt number is used as the surface convective condition in the solid body model, as presented by Culham and Yovanovich (1987). The two solutions are coupled using an iterative procedure to give a unique temperature profile at the fluid-solid interface which simultaneously satisfies the governing equations in both the fluid and the solid domains.

Parametric Analysis

The basic parameters used in the governing equations and the boundary conditions can be expressed in a dimensionless form as follows

$$x^* = x/L \tag{19} \qquad z^* = z/L \tag{20}$$
$$u^* = u/u_{ref} \tag{21} \qquad w^* = w/u_{ref} \tag{22}$$
$$t^* = t/L \tag{23} \qquad \theta = (T - T_\infty)/\Delta T_{ref} \tag{24}$$

where

$$u_{ref} = \alpha/L \tag{25}$$

$$\Delta T_{ref} = \alpha^2/(g\beta L^3) \tag{26}$$

Non-dimensionalizing the governing equations

$$\frac{\partial u^*}{\partial x^*} + \frac{\partial w^*}{\partial z^*} = 0 \tag{27}$$

$$u^* \frac{\partial u^*}{\partial x^*} + w^* \frac{\partial u^*}{\partial z^*} = \mathrm{Pr} \frac{\partial^2 u^*}{\partial (z^*)^2} + \theta \tag{28}$$

$$u^* \frac{\partial \theta}{\partial x^*} + w^* \frac{\partial \theta}{\partial z^*} = \frac{\partial^2 \theta}{\partial (z^*)^2} \tag{29}$$

where the following boundary conditions apply.

$$\text{as } z^* \to \infty \ , \ u^* \to \mathrm{Pe} \ , \ \theta \to 0 \tag{30}$$

$$\text{at } x^* = 0 \ , \ u^* = \mathrm{Pe} \ , \ \theta = 0 \tag{31}$$

$$\text{at } z^* = 0 \ , \ u^* = w^* = 0 \tag{32}$$

where

$$\mathrm{Pe} = \frac{u_\infty \cdot L}{\alpha} \tag{33}$$

The corresponding two-dimensional solid-side equation is written as

$$\frac{k_s t}{k_f L} \left[\frac{\partial^2 \theta}{\partial x^{*2}} + \frac{\partial^2 \theta}{\partial y^{*2}} \right] + \mathrm{Bq}_j - \mathrm{Bq}_r + 2 \frac{\partial \theta}{\partial z^*} \bigg|_{0+} = 0 \tag{34}$$

with

$$\text{at } x^* = 0 \text{ and } 1 \ , \qquad \frac{\partial \theta}{\partial x^*} = 0 \tag{35}$$

$$\text{at } y^* = 0 \text{ and } \frac{W}{L} \ , \qquad \frac{\partial \theta}{\partial y^*} = 0 \tag{36}$$

where Bq is the Boussinesq number defined as

$$\mathrm{Bq} = \frac{g \beta L^4 q}{k_f \alpha^2} \tag{37}$$

with Bq_j based on q_j, and Bq_r based on q_r.

From the above equations, the functional dependency of the dimensionless surface temperature can be written as

$$\theta_w = \theta_w(x^*, y^*, \frac{W}{L}, \frac{k_s t}{k_f L}, \mathrm{Pe}, \mathrm{Pr}, \mathrm{Bq}_j, \mathrm{Bq}_r)$$

This is an implicit non-linear equation due to the radiation heat transfer denoted by Bq_r which contains a fourth-order term of θ_w. Although the above function depends on only six dimensionless parameters, excluding the local positional parameters, the major difficulty in presenting and summarizing the parametric behavior of the surface temperature rests in the fact that one of the input parameters, namely Bq_j, itself is a function of x^* and y^*.

When Bi is greater than 0.1, the three-dimensional solid equation must be solved and the surface temperature depends on an additional parameter as the parameter $k_s t/k_f L$ appears as two isolated components, namely k_s/k_f and t/L.

Default Conditions

Because of the inherent complexity of microelectronic circuit boards and the arrangement of IC packages, an endless combination of configurations could be selected for this study. Instead, a conventional two heat source circuit board, as shown in Fig. 2, will be analyzed, where dimensions, flow conditions and thermophysical properties for the default case are given as

Board	:	$L \times W \times t = 0.2\ (m) \times 0.1\ (m) \times 0.0016\ (m)$
		$k_s = 2\ (W/(m \cdot K))$
		$\epsilon = 0$
Heat Sources	:	$\ell \times \ell = 0.02\ (m) \times 0.02\ (m)$
		$\epsilon = 0$
		$Q_{j_1} = Q_{j_2} = 2\ (W)$
Fluid	:	$k_f = 0.0263\ (W/(m \cdot K))$
(air @ 300 K)		$\nu = 15.89 \times 10^{-6}\ (m^2/s)$
		$\mathrm{Pr} = 0.707$
		$u_\infty = 0.5\ (m/s)$
		$T_\infty = 293\ (K)$
		$T_{sk} = 293\ (K)$

Discussion

A simulation using the default input data is taken as a reference against which all other simulations will be compared. This allows the sensitivity of each of the parameters to be measured against a common measuring stick. Figure 3 shows the surface heat flux, the board temperature and the heat transfer coefficient distribution for our reference conditions, referred to as the default case. Both the applied external flow velocity and the buoyancy driven velocity are in the positive x-direction.

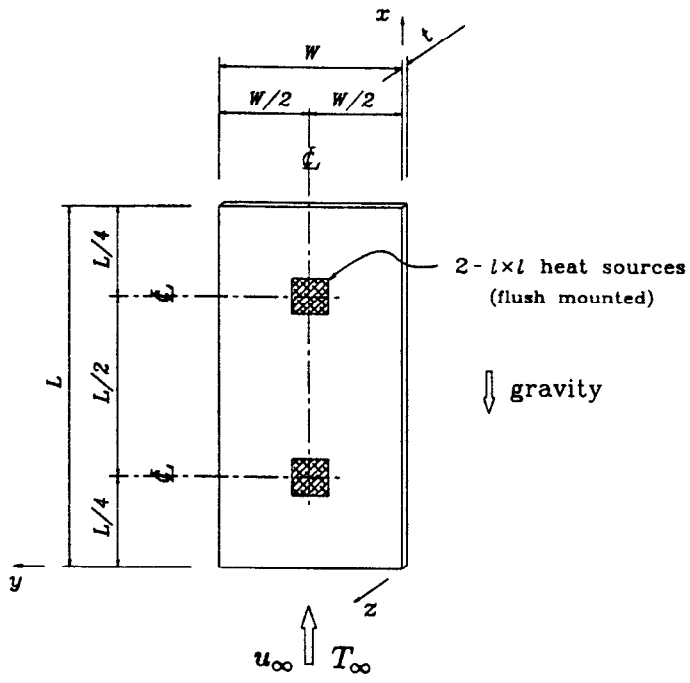

Figure 2: Printed Circuit Board Configuration For the Default Conditions

The Nusselt number for mixed convection can be written in terms of two components representing the Nusselt numbers for forced and natural convection (Churchill, 1977; Shai and Barnea, 1986).

$$\mathrm{Nu}_\mathrm{m}^3 = \mathrm{Nu}_\mathrm{f}^3 + \mathrm{Nu}_\mathrm{n}^3 \tag{38}$$

From laminar flow relationships, the Nusselt number is known to be proportional to the square root of the flow velocity.

$$\mathrm{Nu} \propto \sqrt{u} \tag{39}$$

From the above two equations, an effective mixed convection velocity can be written as

$$u_\mathrm{m}^{1.5} = u_\infty^{1.5} + u_\mathrm{n}^{1.5} \tag{40}$$

where u_∞ is the applied forced flow velocity and u_n can be calculated as in Culham et al., 1991b.

Figure 3a shows the heat flux distribution for the default with the conditions listed above. Given the relatively low board thermal conductivity ($2\ W/(m \cdot K)$) and the low mixed convection velocity ($< 1\ m/s$) the movement of heat throughout the circuit board is impeded and the heat flux distribution is localized in the vicinity of the two heat sources. The relative isolation of the two sources can also be observed in the temperature distribution shown in Fig 3b. In most forced or mixed convection applications where the

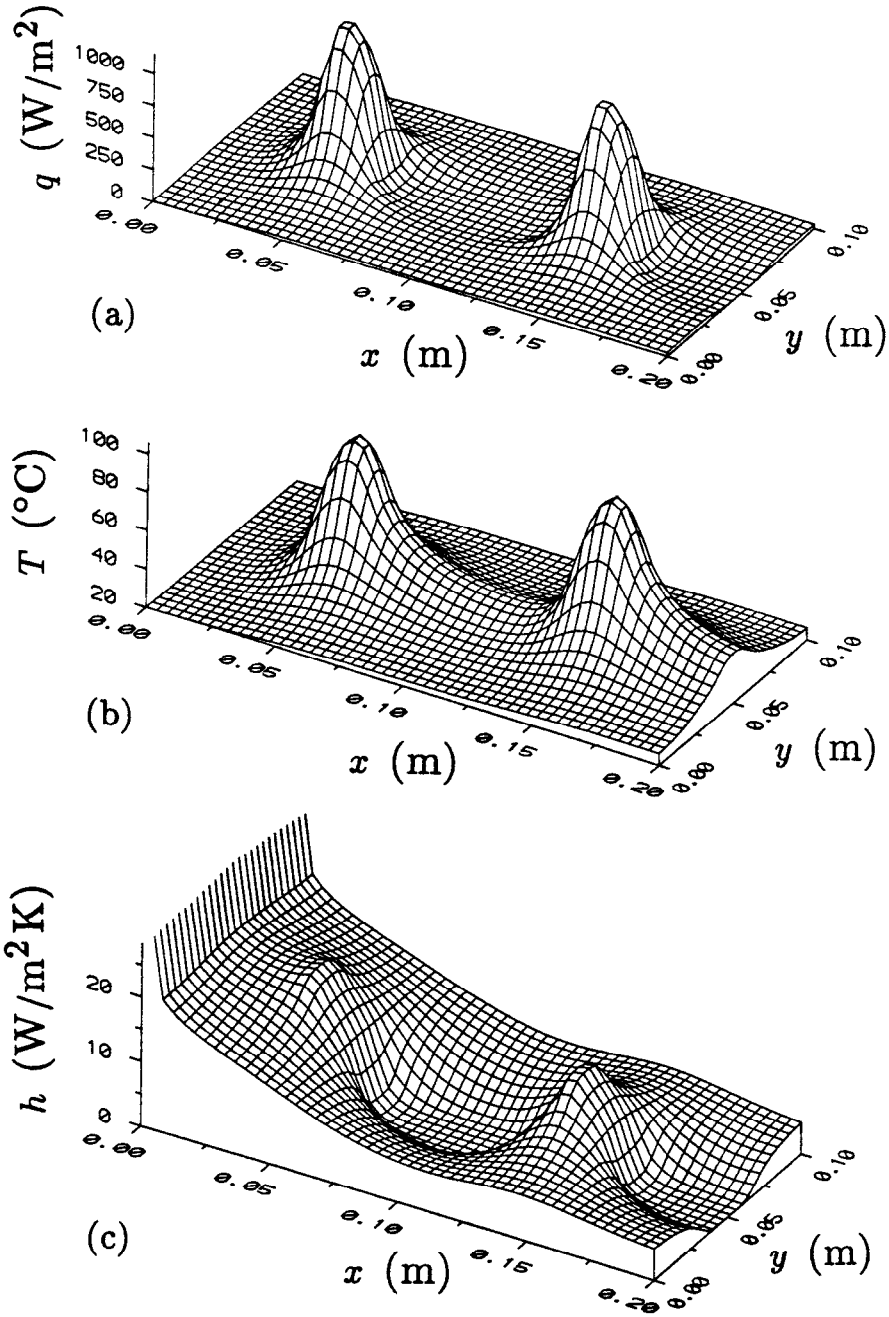

Figure 3: Heat Flux, Temperature and Heat Transfer Coefficient Distributions for the Default Conditions

forced flow is greater than 2 m/s the thermal plume from the first source serves to elevate the temperature of any source downstream. However, as shown in Fig. 3b, the temperature of the second source is only slightly higher than that of the first source, as a direct result of the low mixed convection velocity.

The heat transfer coefficient distribution, shown if Fig. 3c, has a maximum value at the leading edge of the circuit board where the thermal boundary layer is thinnest and the thermal resistance is low. The heat transfer coefficient rises at the leading edge of each source and then falls to near zero within the wake of the heat source, where the boundary layer grows very rapidly, thus increasing the thermal resistance. The edges of the heat sources, parallel to the flow direction offer an alternate heat flow path of lower resistance, as shown in Fig. 3c. Therefore the heat tends to flow within the circuit board perpendicular to the flow direction, showing the most pronounced increase immediately downstream of the heat sources.

Although the heat transfer coefficient distribution is shown over the full range of x and y in Fig. 3c, it is not defined at $x = 0$ and at $y = 0$ or $y = W$. The heat transfer coefficient is a useful tool for estimating the local convective potential, but it should be remembered that the heat transfer coefficient is a derived quantity and is not meaningful over the full domain of x and y.

The design parameters selected to be examined in this study are circuit board thermal conductivity, the surface emissivity of the circuit board, the externally applied flow component of the mixed convection velocity and the heat input to the sources. Each of these parameters will have a direct effect on the thermal resistance of either the boundary layer, the circuit board or both and an indirect influence on the velocity component induced as a result of buoyancy driven flow. To fully account for the complex interaction of each of these parameters in the presence of conjugate mixed convection, a model such as META must be used. Fluid-side models which dismiss the conduction effects within a printed circuit board or solid-side models which rely on boundary layer correlations do not adequately represent the interaction between fluid and solid domains.

Figures 4 - 7 show the effect the control parameters have on dimensionless temperature. Temperature profiles are taken along the centerline of the packages in the positive x direction. In each instance a single parameter is varied, and the other default parameters are maintained.

Thermal Conductivity

The conduction of heat within a printed circuit board is described by Laplace's equation, as given in Eq. (8), which leads to the fin equation, as given in Eq. (18), when the two-dimensional solid model is used. As seen in Eq. (18), the thermal conductivity of the solid, k_s, must be considered in the solution process, and it has a strong impact on the distribution of heat and therefore the distribution of temperature.

Typically, a circuit board consists of alternating layers of highly conductive tracking material, usually copper, separated by a low conductivity, insulating material such as fiberglass-epoxy. Thermal modeling of laminated materials can be accomplished in one of two ways. A more exact, but more complicated method is to treat each layer individually as a homogeneous substance. The temperature fields of the individual layers are coupled through appropriate boundary conditions at the interfaces, allowing a temperature profile of the full cross section to be obtained. Secondly, a more practical method of determining the temperature profile of a laminated material is to calculate an effective thermal conductivity, based on the geometric mean (Lemczyk et al., 1991) of the component thermal conductivities calculated using the series and parallel resistive paths within the laminates. The following discussion of thermal conductivity assumes

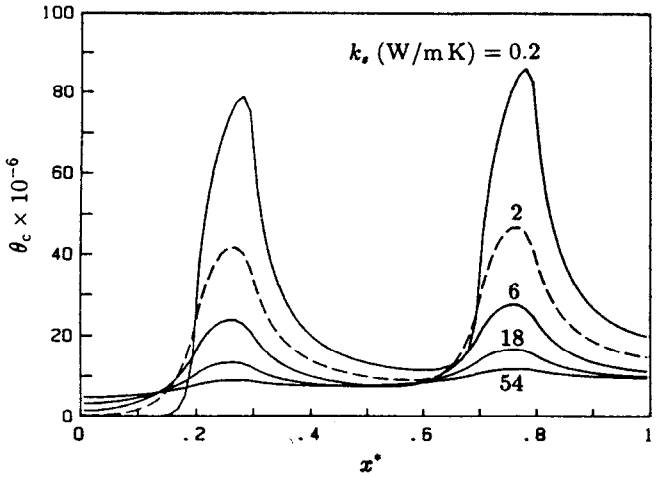

Figure 4: Centerline Temperature Profile Showing the Effect of Changes in Board Thermal Conductivity, k_s, from 0.2 to 54 $W/(m \cdot K)$

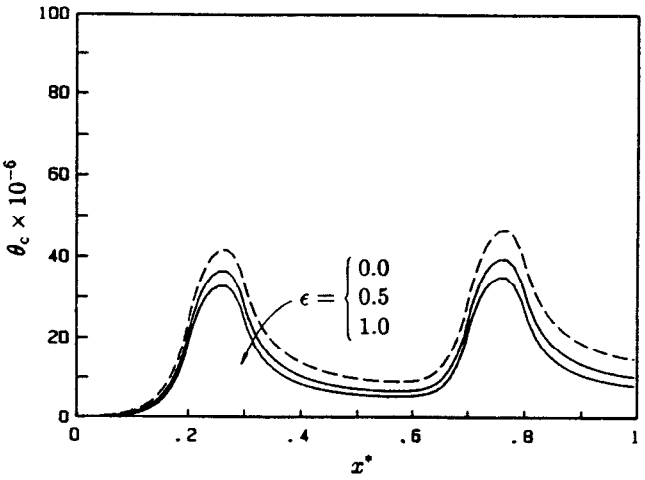

Figure 5: Centerline Temperature Profile Showing the Effect of Changes in Board Emissivity, ϵ from 0 to 1

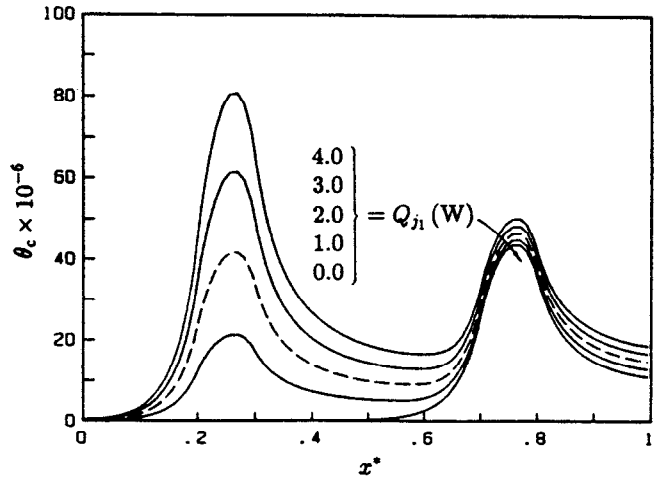

Figure 6: Centerline Temperature Profile Showing the Effect of Changes in Power Level of the Upstream Heat Source, Q_{j_1}, from 0 to 4 W

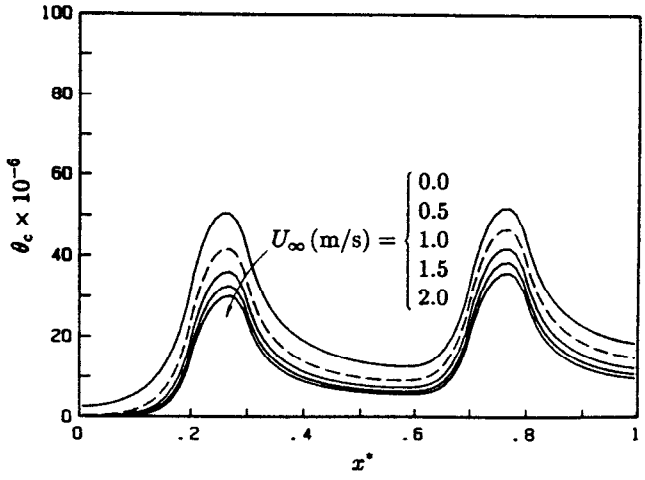

Figure 7: Centerline Temperature Profile Showing the Effect of Changes in the Applied Velocity, u_∞, from 0 to 2 m/s

a single homogeneous value for the entire circuit board.

The thermal conductivity of the circuit board is one of the most sensitive parameters available in the control of peak circuit board temperatures, as shown in Fig. 4. As the thermal conductivity becomes large the heat flows unrestricted within the solid and in the limit an isothermal condition is attained. Increasing the thermal conductivity is an effective means of reducing localized temperature spikes, however, an increase in thermal conductivity is principally obtained by increasing the copper content of the circuit board, resulting in a significant increase in cost.

Through the use of laboratory experiments and numerical simulation it can be seen that the conduction heat transfer in the solid must be considered even for low conductivity materials, such as plastics and fiberglass ($k_s < 0.5\ W/(m \cdot K)$), found in circuit board constructions. The default case, where $k_s = 2$ W/(m · K), is shown using the dotted line in Fig. 4. The solid lines represent the centerline temperature distribution for circuit board conductivities ranging from 0.2 W/(m · K), which can be used as a lower limit for most plastic materials, to 54.0 W/(m · K), which is significantly larger than the maximum effective conductivity of most multilayered boards (typically the thermal conductivity of a multilayered board is less than 10 W/(m · K)).

Over the range of thermal conductivity found in most multilayered circuit boards a reduction in the peak source temperature of between 50 and 300% can be expected for a ten fold increase in the thermal conductivity. An increase in the thermal conductivity from 0.2 W/(m · K) to 2.0 W/(m · K) would require a heat spreader with a thickness of 0.072 mm (approximately 2 ounces of copper).

Surface Emissivity

Even though circuit board temperatures generally are below 100 °C, the radiative exchange between the board and the surroundings cannot be ignored. Radiative heat dissipation levels of 30% for natural convection (Lee et al., 1991) and 10% for forced convection (Culham et al., 1991a) are not uncommon in microelectronic applications. As shown in Fig. 5, a 25% lower temperature over the sources is obtained when the circuit board is treated as a black body ($\epsilon = 1.0$) as opposed to the default case where the emissivity is set equal to zero. If the sink temperature is approximately equal to the room temperature (293 K), a radiative heat transfer coefficient of between 5-6 $W/m^2 \cdot K$ is obtained over the full range of operating temperatures encountered in a typical circuit board ($\approx$ 293K – 393K). In examining the convective heat transfer coefficient distribution in Fig. 3c, it is readily apparent that the radiative heat transfer coefficient may be 25% at the sources but in locations such as those immediately downstream of the sources, the radiative heat exchange is essentially the only means of heat rejection. Neglecting the radiative heat exchange in the thermal analysis of a microelectronic circuit board can give misleading results especially in cases where the circuit board is isolated and radiating to free space or a surrounding cabinet.

Source Strength

Figure 6 shows the effect on the centerline temperature resulting from a change in the power applied to the upstream heat source. The power to the downstream heat source is maintained at 2 W, as in the default case. As would be expected, increasing the power of the upstream heat source results in a significant increase in the temperature at the upstream heat source itself, but because of the mixed convection plume

and the conduction within the board, heat is also carried downstream in the boundary layer, heating everything in its wake.

In doubling the power of the upstream heat source from 2 W to 4 W the dimensionless temperature of the upstream heat sources rises by slightly less than a factor of two. This indicates the predominant role of forced convection, where the linear behavior of power in forced convection should lead to a 1:1 relationship between power and temperature. But because the mixed convection velocity also includes a buoyancy driven component, the temperature rise of the upstream heat source is lower than an equivalent forced convection situation. The temperature rise over the downstream heat source due to upstream heating effects is approximately 8% greater than in the default situation where the power levels of the two sources were maintained at 2 W each. Increasing the power of the upstream heat source both helps and hinders the cooling of components in its wake. First as discussed above, the heat rejected over the upstream heat source raises the temperature level within the boundary layer resulting in a temperature rise of all components in the wake of the upstream heat source. However, the increase in heat flux and in turn temperature at upstream locations also results in an increase in the velocity component due to buoyancy driven flow. This added velocity component helps lower temperatures of components with the wake of the upstream heat source but the overall result is approximately an 8% increase in temperature at the downstream heat source due to a 100% increase in the power applied to the upstream heat source.

Air Flow Velocity

The board temperature is affected by both the applied forced flow velocity and the buoyancy driven natural convection velocity as shown in Eq. (40). By calculating a velocity component which is directly attributed to natural convection effects (Culham et al., 1991b), an effective mixed convection velocity can be obtained which allows the momentum and energy equations to be used in their uncoupled form, similar to a conventional forced convection analysis.

Although increasing the velocity can be an effective means of controlling temperature, it can be seen in Fig. 7 that the biggest advantage is obtained for velocities less than 2 m/s while for velocities greater than 2 m/s the reduction in board temperature diminishes. In addition to the diminishing returns attained for higher velocities, a practical limit of flow velocity of approximately 5 m/s is mandated for most office environments due to noise constraints.

Source Location

Figure 8 shows the relationship between the dimensionless temperature of the second source when the first source is moved from the leading edge to the trailing edge of the board.

When $\tilde{d}$, the distance between the centerline of the two heat sources divided by the source length (ℓ) is equal to zero, the two sources overlap, and the temperature distribution is identical to a single source with twice the heat dissipation. As shown in Culham et al., 1991b the forced convection problem is linear and the resultant temperature is twice that of $\Delta T_{2,0}$.

$$\phi = \frac{\Delta T_2 - \Delta T_{2,0}}{\Delta T_{2,0}} \tag{41}$$

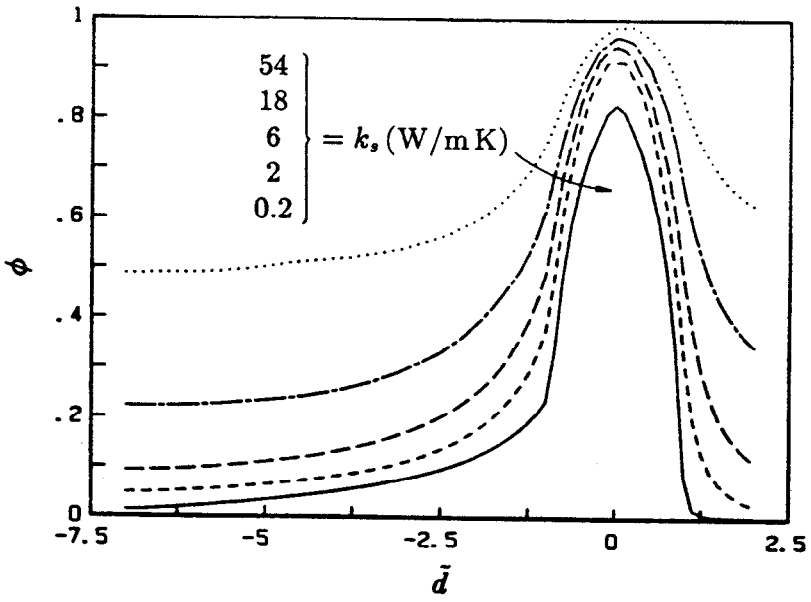

Figure 8: **Dimensionless Average Temperature of the Downstream Heat Source as a Function of the Position of the Upstream Heat Source**

where $\Delta T_{2,0}$ is the average temperature excess of the second source when the second source is the only source on the board. In the mixed convection case shown here the temperature is slightly less than in the forced convection case because the buoyancy induced flow enhances the forced flow to improve heat transfer and thereby lower board temperatures.

Parameter Summary

Figure 9 is a summary of the effects of the flow velocity, surface emissivity and thermal conductivity of the circuit board and the source strength of the upstream source on the heat transfer effectiveness of the downstream source as measured by the average Nusselt number of the downstream source, written as

$$\mathrm{Nu}_2 = \frac{Q_{j_2}}{(\overline{T}_2 - T_\infty)k_f \ell} \tag{42}$$

The multiple scales along the abscissa are arranged such that the node in the center of the curves corresponds to the default conditions. Therefore the heat transfer effectiveness, as measured at the downstream heat source, can be compared for the range of design conditions discussed herein.

A change in the thermal conductivity leads to the largest change in the Nusselt number, with a change of circuit board conductivity between the default setting of 2 $W/(m \cdot K)$ and a value of 54 $W/(m \cdot K)$ giving a three fold increase in the Nusselt number. As the thermal conductivity is increased beyond 20 $W/(m \cdot K)$ the rate of increase in the Nusselt number slowly diminishes as the thermal resistance in the

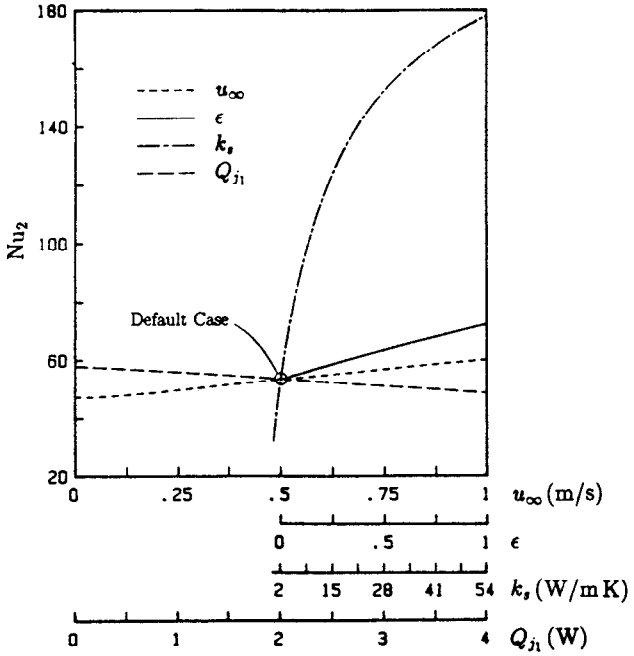

Figure 9: Average Nusselt Number Variation of the Downstream Heat Source as a Function of u_∞, ϵ, k_s, and Q_{j_1}

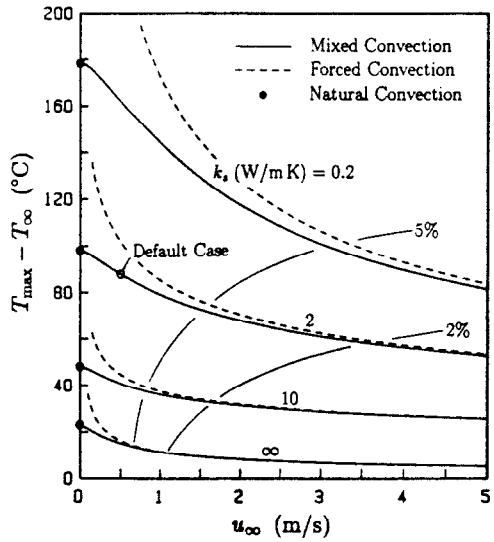

Figure 10: Maximum Board Temperature as a Result of Mixed and Forced Convection Over a Range of Applied Flow Velocities, u_∞, Between 0 and 5 m/s

boundary layer begins to increase. A change in the emissivity between 0 and 1 provides an increase in the Nusselt number of approximately 50%, which is twice the change in Nusselt number incurred by increasing the applied flow velocity from 0.5 m/s to 1.0 m/s. An increase in the heat flux of the first source reduces the Nusselt number of the second source by 10 - 15% due to the wake effect through the boundary layer.

Figure 10 shows the relative effect of mixed convection compared to pure forced convection over a range of applied flow velocities between 0 (natural convection) and 5 m/s and a range of circuit board thermal conductivities between 0.2 $W/(m \cdot K)$ and the isothermal board case where the conductivity is infinite. The lines which are nominally vertical, indicate the locust of points where a 2% and 5% difference between the mixed and forced convection results occur. Knowing the conductivity of the circuit board, the significance of mixed convection can be measured against the applied forced velocity.

Figure 11 relates the heat dissipated directly from the heat sources by the various modes of heat transfer, i.e., conduction, convection and radiation, for a range of board thermal conductivities between 0 and 10 $W/(m \cdot K)$. Three levels of emissivity are presented for each case.

The radiative component of the dissipated heat is approximately 5% for thermal conductivities greater than 3 $W/(m \cdot K)$ but can be in the range of 15% for plastic substrates with thermal conductivities of 0.2 $W/(m \cdot K)$.

When the thermal conductivity of the board is small, the resistance to heat flow under the source is greater than the thermal resistance of the boundary layer and the heat dissipated by convection dominates. However, at a thermal conductivity of approximately 1.0 $W/(m \cdot K)$ the resistance between the

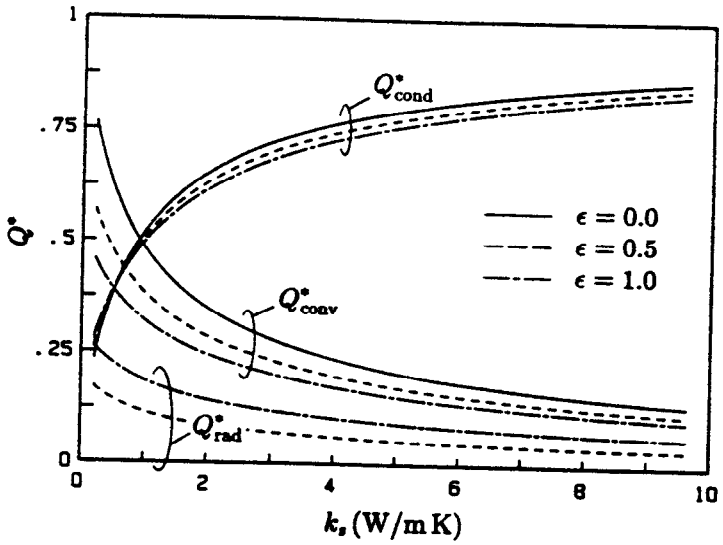

Figure 11: **Dimensionless Heat Dissipation from the Downstream Heat Source by Means of Conduction, Convection and Radiation**

boundary layer and the board are equivalent and the two modes of heat transfer are essentially of equivalent magnitude. For board conductivities greater than 1.0 $W/(m \cdot K)$ the conduction within the board dominates.

The convective fraction decreases with increasing conductivity primarily because the resistance within the boundary layer is greater than the resistance in the board.

Concluding Remarks

Conjugate heat transfer problems of the type described in the previous sections can be extremely complex due to the interaction of the fluid and solid domains and the necessity for the governing equations in each domain to be satisfied simultaneously. Studies of this type are useful for observing the relative importance of basic design parameters in respect to the role they have in controlling local circuit board temperatures. The ability to analyze problems of a general nature can only be accomplished by conducting extensive laboratory experiments, which can be time consuming and extremely expensive to perform, or through the use of a general purpose conjugate model, such as META.

Acknowledgments

The authors wish to thank the Natural Sciences and Engineering Research Council of Canada for financial support under CRD contract 661-062/88.

References

Churchill, S.W., 1977, "A Comprehensive Correlating Equation for Laminar, Assisting, Forced and Free Convection," *AIChE Journal*, Vol. 23, pp 10-16.

Culham, J.R, Lee, S. and Yovanovich, M.M., 1991a, "The Effect of Common Design Parameters on the Thermal Performance of Microelectronic Equipment: Part II - Forced Convection," ASME National Heat Transfer Conference, Minneapolis, MN, July 28-31.

Culham, J.R., Lemczyk, T.F., Lee, S. and Yovanovich, M.M., 1991b, "META - A Conjugate Heat Transfer Model For Cooling of Circuit Boards With Arbitrarily Located Heat Sources," ASME National Heat Transfer Conference, Minneapolis, Minnesota, July 28-31.

Culham, J.R. and Yovanovich, M.M., 1987, "Non-Iterative Technique for Computing Temperature Distributions in Flat Plates with Distributed Sources and Convective Cooling", Second ASME–JSME Thermal Engineering Joint Conference, Honolulu, Hawaii, March 22–27.

Lee, S., Culham, J.R and Yovanovich, M.M., 1991, "The Effect of Common Design Parameters on the Thermal Performance of Microelectronic Equipment: Part I - Natural Convection," ASME National Heat Transfer Conference, Minneapolis, MN, July 28-31.

Lee, S. and Yovanovich, M.M., 1991, "Linearization of Natural Convection From a Vertical Plate With Arbitrary Heat Flux Distributions," ASME Winter Annual Meeting, Atlanta, GA, December 1-6.

Lemczyk, T.F., Mack, B.F., Culham, J.R. and Yovanovich, M.M., 1991, "PCB Trace Thermal Analysis and Effective Conductivity," 7th Annual IEEE Semi Conductor Temperature and Thermal Management Symposium (SEMI-THERM), Phoenix, AZ, February.

Shai, I. and Barnea, Y., 1986, "Simple Analysis of Mixed Convection With Uniform Heat Flux," *International Journal of Heat and Mass Transfer*, Vol. 29, pp 1139-1147.